Always-Dual-Path Hybrid DC-DC Converter Achieving High Efficiency at Around 2:1 Step-Down Ratio

Katsuhiro Hata[1], Yang Jiang[1, 2], Man-Kay Law[2], and Makoto Takamiya[1]
[1]The University of Tokyo, Tokyo, Japan
[2]University of Macau, Macau, China
E-mail: khata@iis.u-tokyo.ac.jp

***Abstract*— An always-dual-path hybrid (ADPH) DC-DC converter using one inductor and two flying capacitors with the step-down ratio from 3:1 to 1:1 is proposed to achieve high efficiency at the commonly used 2:1 step-down ratio by reducing the inductor current. The proposed ADPH converter is designed for a 24 V-to-13 V bus converter for truck auxiliary equipment. In the measurement, the peak efficiency of the proposed 24 V-to-13 V converter is 97.4 % at 146 W, and the inductor conduction loss is reduced by 67.2 % by reducing the inductor DC current by 42.7 %.**

***Keywords*— DC-DC converter, Step-down converter, Hybrid converter, Always-dual-path, Equivalent series resistance (ESR)**

I. Introduction

Hybrid step-down DC-DC converters [1-11] combining a buck converter and a switched capacitor DC-DC converter could overcome the trade-off between the efficiency and the form factor of the commonly used buck converter. In addition, [12-15] reported unique hybrid step-down DC-DC converters, where an inductor is indirectly connected to the output and the output current is divided into a dual-path (inductor and capacitor path). Hence, the converters [12-15] can reduce the conduction loss due to the ESR of the inductor. This is quite beneficial when the inductor loss dominates at heavy load conditions. The converters [12-15], however, cannot be used in the applications requiring around 2:1 step-down ratio, because the step-down ratio with two circuit states is limited to either more than half or less than half [12-15]. Meanwhile, the conventional 3-level buck converters require different control schemes to operate across a half step-down ratio [16, 17], which complicates the controller. In addition, the inductor current in a 3-level converter equals to the output current, which results in a high DCR loss in heavy load conditions.

To solve the problems, an always-dual-path hybrid (ADPH) DC-DC converter using one inductor and two flying capacitors with only two circuit states and the step-down ratio from 3:1 to 1:1 is proposed for the first time. The proposed ADPH converter can dramatically reduce inductor conduction loss and achieve high efficiency, especially at around 2:1 step-down ratio. In this paper, operation principle and basic characteristic of the proposed ADPH converter are described analytically. Also, the proposed ADPH converter is designed for a 24 V-to-13 V bus converter for truck auxiliary equipment and is measured using a prototype.

II. Proposed Always-Dual-Path Hybrid Converter

A. Circuit operation and voltage conversion ratio

Fig. 1 shows the proposed ADPH converter topology using one inductor and two flying capacitors. As shown in Figs. 2 (a) and (b), the converter has two circuit states. In both states, the output current is always divided into a dual path.

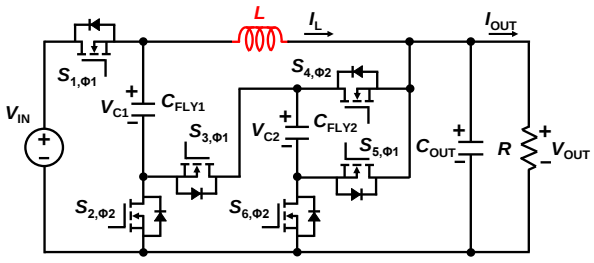

Fig. 1. Proposed always-dual-path hybrid (ADPH) converter.

First, the voltages $V_{C1,2}$ in the flying capacitors $C_{FLY1,2}$ are obtained from the steady-state analysis of the proposed ADPH converter. Assuming that the output voltage V_{OUT} is well regulated and its ripple is small enough, the flying capacitor voltages V_{C1} and V_{C2} described as follows:

$$\begin{aligned} V_{C1} &= V_{IN} - V_{C2} - V_{OUT} \\ &= V_{IN} - 2V_{OUT} \end{aligned} \quad (1)$$

$$V_{C2} = V_{OUT}. \quad (2)$$

where, V_{IN} represents the input voltage and its value is assumed to remain unchanged in a short period of time.

Next, the voltage conversion ratio M of the proposed ADPH converter is derived from the inductor voltage V_L in each circuit state. By considering voltage-second balance in L, the voltage conversion ratio M can be obtained as follows:

$$\begin{aligned} 0 &= \langle V_L \rangle \\ &= (V_{IN} - V_{OUT})DT_{SW} + (V_{C1} - V_{OUT})(1-D)T_{SW} \\ &= (V_{IN} - V_{OUT})DT_{SW} - (V_{IN} - 3V_{OUT})(1-D)T_{SW} \end{aligned} \quad (3)$$

$$\Leftrightarrow \frac{V_{OUT}}{V_{IN}} = \frac{1}{3-2D}$$

$$M = \frac{V_{OUT}}{V_{IN}} = \frac{1}{3-2D} \quad (4)$$

$$D = \frac{3M-1}{2M} \quad (5)$$

where, $\langle V_L \rangle$, D, and T_{SW} are the average of inductor voltage, the duty cycle, and the switching period, respectively.

Fig. 3 illustrates M as a function of D in the proposed ADPH converter in contrast with the conventional buck converter. The step-down operation range of the proposed ADPH converter is from 3:1 to 1:1. In this study, the design

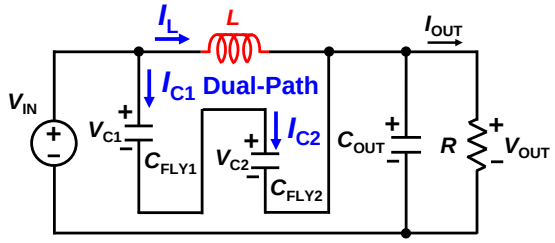

(a) State 1

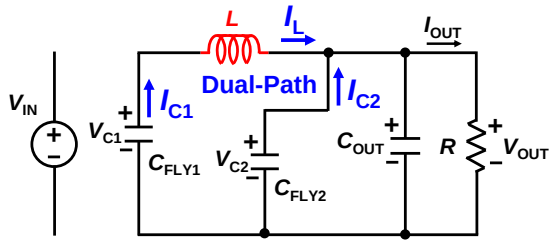

(b) State 2

Fig. 2. Two circuit states in the proposed ADPH converter.

target is set to $0.4 < M < 0.6$, because the target application is a 24 V-to-13 V bus converter for truck auxiliary equipment and the input voltage is assumed to change from 22 V to 32 V depending on the battery voltage.

B. Inductor DC current

To show that the proposed ADPH converter can reduce the inductor current I_L compared to the conventional buck converter, the relationship between I_L and the output current I_{OUT} in the proposed ADPH converter is analyzed.

I_L and I_{OUT} are defined as the periodic average current flowing to the output and through the inductor, and from the charge balance in C_{FLY1} and C_{FLY2} at periodic steady state, the output current I_{OUT} and the capacitor currents I_{C1} and I_{C2} are described as follows:

$$I_{OUT} = \left(DI_L + I_{C1}\right) + \left\{\left(1-D\right)I_L + I_{C2}\right\} \tag{6}$$

$$I_{C1} = I_{C2} = \left(1-D\right)I_L. \tag{7}$$

By combining (6) and (7), the relationship between I_L and I_{OUT} in the proposed ADPH converter can be expressed as follows:

$$\begin{aligned} & I_{OUT} = \left(3-2D\right)I_L \\ \Leftrightarrow\ & I_L = \frac{1}{3-2D} I_{OUT} = MI_{OUT} \end{aligned} \tag{8}$$

As a result, the inductor DC currents of the proposed converter and the conventional converter can be summarized as follows:

$$I_{L,DC,ADPH} = MI_{OUT} \tag{9}$$

$$I_{L,DC,Buck} = I_{OUT}. \tag{10}$$

Consequently, the inductor DC current of the proposed ADPH converter $I_{L,DCADPH}$ can be reduced compared with that of the buck converter $I_{L,buck}$ as follows:

$$K_{DC} = \frac{I_{L,DC,ADPH}}{I_{L,DC,Buck}} = M. \tag{11}$$

The Inductor DC current ratio K_{DC} is indicated in Fig. 4.

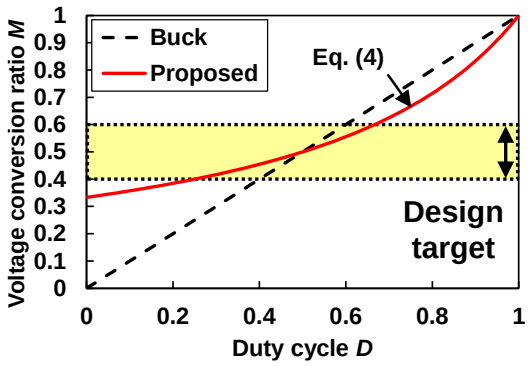

Fig. 3. Voltage conversion ratio M vs. duty cycle D.

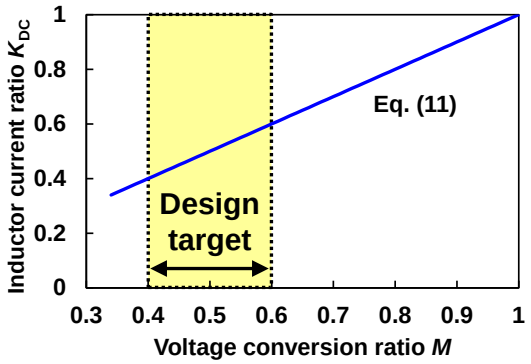

Fig. 4. Inductor DC current ratio K_{DC} vs. voltage conversion ratio M.

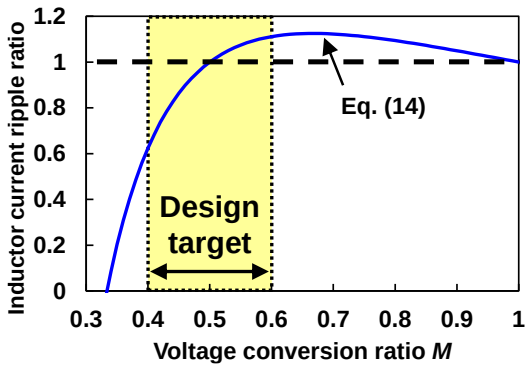

Fig. 5. Inductor current ripple ratio K_{ripple} vs. voltage conversion ratio M.

C. Inductor current ripple

Additionally, in order to compare the inductor conduction loss of the proposed ADPH converter and the conventional buck converter, the inductor current ripple is also analyzed.

From the inductor voltage V_L in the circuit state 1, which is shown in Fig. 2(a), the inductor current ripple of the proposed ADPH converter $\Delta I_{L,ADPH}$ is obtained as follows:

$$\begin{aligned} \Delta I_{L,ADPH} &= \frac{DT_{SW}\left(V_{IN} - V_{OUT}\right)}{L} \\ &= \frac{2D\left(1-D\right)V_{OUT}}{Lf_{SW}} \\ &= \frac{V_{OUT}}{Lf_{SW}} \frac{\left(3M-1\right)\left(1-M\right)}{2M^2}. \end{aligned} \tag{12}$$

where, f_{SW} is the switching frequency. Similarly, the inductor current ripple of the conventional buck converter $\Delta I_{L,Buck}$ is also described as follows:

$$\Delta I_{L,Buck} = \frac{V_{OUT}}{L f_{SW}}(1-M). \tag{13}$$

Therefore, the inductor current ripple ratio K_{ripple} is expressed by the following equation and is shown in Fig. 5.

$$K_{ripple} = \frac{\Delta I_{L,ADPH}}{\Delta I_{L,Buck}} = \frac{3M-1}{2M^2} \tag{14}$$

III. Loss Analysis

A. Inductor conduction loss

From the inductor DC current and ripple analyses, the inductor conduction loss $P_{L,RMS}$ can be calculated as follows:

$$P_{L,RMS} = R_{L,DC} I_{L,RMS}^2 \tag{15}$$

$$I_{L,RMS}^2 = I_{L,DC}^2 + \frac{\Delta i_L^2}{12} \tag{16}$$

where, $R_{L,DC}$ is the parasitic DC resistance of the inductor.

If the inductor current ripple ΔI_L is sufficiently small with respect to the inductor DC current $I_{L,DC}$, the second term in (16) can be ignored. In addition, as shown in Fig. 5, the inductor current ripple ratio between the proposed ADPH converter and the conventional buck converter is around 1, so the conduction loss caused by ΔI_L is not considered in this study. As a result, the inductor conduction loss $P_{L,DC}$ is simplified as follows:

$$P_{L,DC} = R_{L,DC} I_{L,DC}^2. \tag{17}$$

From (9) and (10), the inductor conduction losses of the proposed ADPH converter $P_{L,DC,ADPH}$ and the conventional buck converter $P_{L,DC,Buck}$ are obtained as follows:

$$P_{L,DC,ADPH} = R_{L,DC} I_{L,DC,ADPH}^2 = M^2 R_{L,DC} I_{OUT}^2 \tag{18}$$

$$P_{L,DC,Buck} = R_{L,DC} I_{L,DC,Buck}^2 = R_{L,DC} I_{OUT}^2. \tag{19}$$

Therefore, the proposed ADPH converter can reduce the inductor conduction loss $P_{L,DC}$ in proportion to the square of the voltage conversion ratio M compared to the conventional buck converter, and this reduction ratio $K_{L,DC}$ can be described as follows:

$$K_{L,DC} = \frac{P_{L,DC,ADPH}}{P_{L,DC,Buck}} = M^2. \tag{20}$$

B. Switch conduction loss

While the proposed ADPH converter can reduce the inductor DC current, the number of power switches is increased, so it is necessary to analyze the switch conduction loss. Assuming that the on-state resistance of the power switch does not change significantly, the switch conduction loss can be calculated from the current flowing through each switch.

Assuming that the inductor current ripple is small enough, the current flowing through each switch is obtained as follows:

$$I_{S1} = I_L + I_{C1,\phi 1} \tag{21}$$

$$I_{S2} = I_{C1,\phi 2} \tag{22}$$

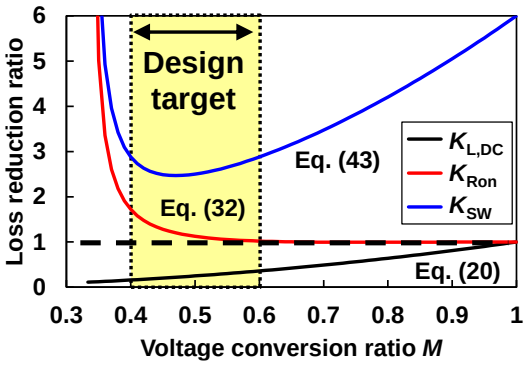

Fig. 6. Loss reduction ratios $K_{L,DC}$, K_{Ron}, K_{SW} vs. voltage conversionratio M.

$$I_{S3} = I_{C1,\phi 1} \tag{23}$$

$$I_{S4} = I_{C1,\phi 2} \tag{24}$$

$$I_{S5} = I_{C1,\phi 1} \tag{25}$$

$$I_{S6} = I_{C1,\phi 2} \tag{26}$$

where, $I_{C,\Phi 1}$ and $I_{C,\Phi 2}$ are the flying capacitor currents of each circuit state and they are described as follows:

$$I_{C1,\phi 1} = I_{C2,\phi 1} = \frac{1-D}{D} I_L \tag{27}$$

$$I_{C1,\phi 2} = I_{C2,\phi 2} = I_L. \tag{28}$$

From these results and the operating conditions of each circuit state, the switch conduction loss P_{Ron} is derived as follows:

$$\begin{aligned} P_{Ron} &= D\left(R_{S1} I_{S1}^2 + R_{S3} I_{S3}^2 + R_{S5} I_{S5}^2\right) \\ &\quad + (1-D)\left(R_{S2} I_{S2}^2 + R_{S4} I_{S4}^2 + R_{S6} I_{S6}^2\right) \\ &= \left\{ \frac{1}{D} R_{S1} + \frac{(1-D)^2}{D}\left(R_{S3} + R_{S5}\right) \right. \\ &\quad \left. + (1-D)\left(R_{S2} + R_{S4} + R_{S6}\right) \right\} I_L^2 \end{aligned} \tag{29}$$

For design simplicity, assuming that the same device is used for all power switches employ, i.e. $R_{SW} = R_{S1} = R_{S2} = R_{S3} = R_{S4} = R_{S5} = R_{S6}$, the switch conduction loss of the proposed ADPH converter $P_{Ron,ADPH}$ can be described as follows:

$$\begin{aligned} P_{Ron,ADPH} &= \left(\frac{3}{D} - 1 - D\right) R_{SW} I_L^2 \\ &= \frac{-3M^3 + 8M^2 - M}{6M - 2} R_{SW} I_{OUT}^2. \end{aligned} \tag{30}$$

Similarly, the switch conduction loss of the conventional buck converter $P_{Ron,Buck}$ is obtained as follows:

$$P_{Ron,Buck} = D R_{SW} I_{OUT}^2 + (1-D) R_{SW} I_{OUT}^2 = R_{SW} I_{OUT}^2. \tag{31}$$

As a result, the switch conduction loss ratio between the proposed ADPH and conventional buck converters K_{Ron} can be derived as follows:

$$K_{Ron} = \frac{P_{Ron,ADPH}}{P_{Ron,Buck}} = \frac{-3M^3 + 8M^2 - M}{6M - 2}. \tag{32}$$

C. Switching loss

Since an increase in the number of power switches also leads to an increase in switching loss, this study conducts a simple analysis to confirm this tendency.

First, the sustained voltage of each switch is considered assuming a small ripple of each capacitor voltage. Since each capacitor voltage is given by (1) and (2), the sustained voltage for the power switches during their turned-off state is obtained as follows:

$$V_{S1} = V_{S2} = 2V_{OUT} \tag{33}$$

$$V_{S3} = V_{S4} = V_{S5} = V_{S6} = V_{OUT}. \tag{34}$$

Since the current flowing through each power switch is calculated from (21) – (28) with small ripple assumption, each switching loss can be derived as follows:

$$P_{SW1} = \frac{1}{2} f_{SW} V_{S1} I_{S1} (t_{ON} + t_{OFF}) = \frac{1}{D} f_{SW} V_{OUT} I_L (t_{ON} + t_{OFF}) \tag{35}$$

$$P_{SW2} = \frac{1}{2} f_{SW} V_{S2} I_{S2} (t_{ON} + t_{OFF}) = f_{SW} V_{OUT} I_L (t_{ON} + t_{OFF}) \tag{36}$$

$$P_{SW3} = \frac{1}{2} f_{SW} V_{S3} I_{S3} (t_{ON} + t_{OFF}) = \frac{1-D}{2D} f_{SW} V_{OUT} I_L (t_{ON} + t_{OFF}) \tag{37}$$

$$P_{SW4} = \frac{1}{2} f_{SW} V_{S4} I_{S4} (t_{ON} + t_{OFF}) = \frac{1}{2} f_{SW} V_{OUT} I_L (t_{ON} + t_{OFF}) \tag{38}$$

$$P_{SW5} = \frac{1}{2} f_{SW} V_{S5} I_{S5} (t_{ON} + t_{OFF}) = \frac{1-D}{2D} f_{SW} V_{OUT} I_L (t_{ON} + t_{OFF}) \tag{39}$$

$$P_{SW6} = \frac{1}{2} f_{SW} V_{S6} I_{S6} (t_{ON} + t_{OFF}) = \frac{1}{2} f_{SW} V_{OUT} I_L (t_{ON} + t_{OFF}). \tag{40}$$

where, t_{ON} and t_{OFF} are the turn-on time and turn-off time, respectively. Here, since a dead time is not considered as a basic analysis, all switching losses are calculated as hard switching. If soft switching can be achieved, the switching loss can be reduced, but its implementation is a future study.

From these results, the switching loss of the proposed ADPH converter $P_{SW,ADPH}$ can be obtained as follows:

$$P_{SW,ADPH} = \frac{14M-2}{3M-1} f_{SW} V_{OUT} I_L (t_{ON} + t_{OFF}) = \frac{14M^3 - 2M^2}{3M-1} f_{SW} V_{IN} I_{OUT} (t_{ON} + t_{OFF}). \tag{41}$$

Similarly, the switching loss of the conventional buck converter $P_{SW,Buck}$ is calculated as follows:

$$P_{SW,Buck} = \frac{1}{2} f_{SW} V_{IN} I_{OUT} (t_{ON} + t_{OFF}) + \frac{1}{2} f_{SW} V_{IN} I_{OUT} (t_{ON} + t_{OFF}) = f_{SW} V_{IN} I_{OUT} (t_{ON} + t_{OFF}) \tag{42}$$

Although the lower switch of the conventional buck converter achieves soft switching in a synchronous rectification, its switching loss is described as hard switching because the dead time period is not considered in this study.

From these analyses, the switching loss ratio between the proposed ADPH and conventional buck converters K_{SW} can be obtained as follows:

$$K_{SW} = \frac{P_{SW,ADPH}}{P_{SW,Buck}} = \frac{14M^3 - 2M^2}{3M-1}. \tag{43}$$

Fig. 6 shows the tendency of the loss reduction ratios $K_{L,DC}$, K_{Ron}, K_{SW} in the operating range of the voltage conversion ratio M. Although the proposed ADPH converter can drastically reduce the inductor conduction loss by reducing the inductor DC current, the switch conduction loss and switching loss significantly increase in $M < 0.4$, and the superiority over the conventional buck converter cannot be maintained in this range. Additionally, in $0.6 < M$, the conduction losses have good characteristics, but the increase in the switching loss cannot be ignored. Therefore, the appropriate design target of the proposed ADPH converter is $0.4 < M < 0.6$.

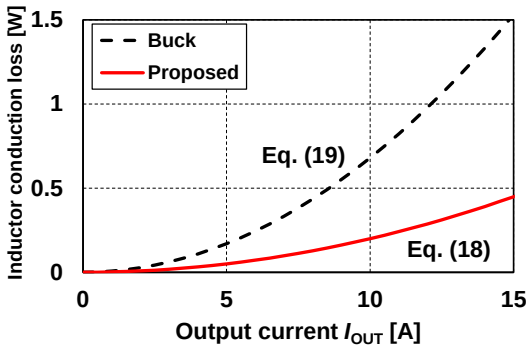

(a) Inductor conduction loss

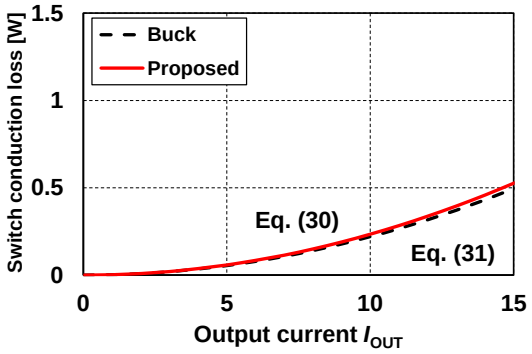

(b) Switch conduction loss

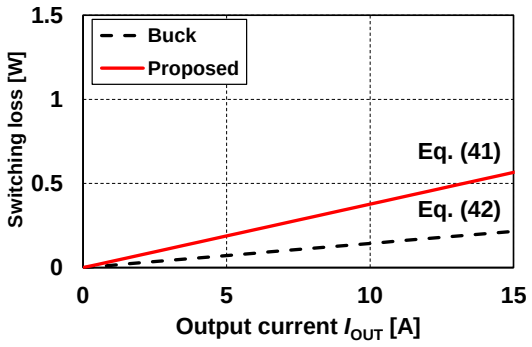

(c) Switching loss

Fig. 7. Loss comparison between proposed ADPH converter and conventional buck converter under conditions of V_{IN} = 24 V, V_{OUT} = 13 V, M = 13/24, $R_{L,DC}$ = 6.8 mΩ, R_{SW} = 2.2 mΩ, f_{SW} = 100 kHz, and (t_{ON} + t_{OFF}) = 6 ns.

D. Case study

In order to compare not only the loss reduction ratios but also the magnitude of losses, the proposed ADPH converter is designed and each loss is calculated. Because the target application is a 24 V-to-13 V bus converter for truck auxiliary equipment, the voltage conversion ratio was set to M = 13/24

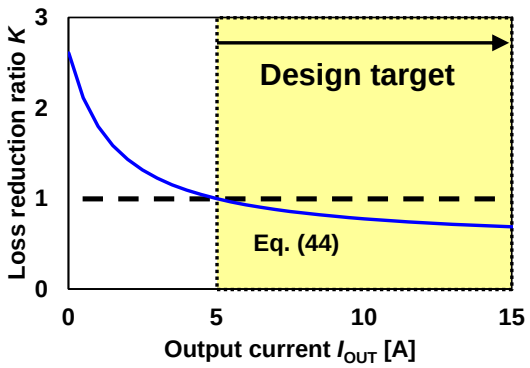

Fig. 8. Loss reduction ratio K under conditions of V_{IN} = 24 V, V_{OUT} = 13 V, M = 13/24, $R_{L,DC}$ = 6.8 mΩ, R_{SW} = 2.2 mΩ, f_{SW} = 100 kHz, and (t_{ON} + t_{OFF}) = 6 ns.

and the rated voltage of each switch was selected as 40 V or higher. Other selected components are listed in TABLE I.

Fig. 7 shows the loss comparison between the proposed ADPH converter and the conventional buck converter under conditions of V_{IN} = 24 V, V_{OUT} = 13 V, M = 13/24, $R_{L,DC}$ = 6.8 mΩ, R_{SW} = 2.2 mΩ, f_{SW} = 100 kHz, and (t_{ON} + t_{OFF}) = 6 ns. In the range where the output current is small, the switch loss is dominant over the inductor conduction loss, but the inductor conduction loss increases significantly as the output current increases, so the proposed ADPH converter is superior to the conventional buck converter.

To consider the loss reduction ratio corresponding to changes in loss distribution, the loss reduction rate K including the inductor conduction loss, the switch conduction loss, and the switching loss at the same time is calculated as follows:

$$K = \frac{P_{L,DC,ADPH} + P_{Ron,ADPH} + P_{SW,ADPH}}{P_{L,DC,Buck} + P_{Ron,Buck} + P_{SW,Buck}}. \quad (44)$$

With the design parameters listed in TABLE I, the loss reduction ratio K is calculated and depicted in Fig. 8. As a result, the proposed ADPH converter offers lower loss than the conventional buck converter when the output current is larger than 5 A.

IV. Experimental Verification

A. Experimental setup

In order to measure the efficiency of the proposed ADPH converter and compare it with the conventional buck converter, the prototype converter was implemented on the 116.8 mm × 61 mm 2-layer PCB as shown in Fig. 9.

The proposed ADPH converter was operated based on the two circuit state shown in Fig. 2. On the other hand, the conventional buck converter was composed of S_1, S_2, L, C_{IN}, and C_{OUT} in Fig. 9. In the buck converter operation, $S_{3\text{-}6}$ and $C_{FLY1,2}$ are removed, and the source of S_1 and the drain of S_2 are connected with a jumper resistor. The conventional buck converter was operated in a synchronous rectification mode.

The efficiency was calculated from the input power and output power, and each power was measured using a power analyzer (PW3390, HIOKI). The inductor DC current was measured by an oscilloscope (MDO34 3-BW-200, Tektronix) with an AC/DC current probe (TPC0030A, Tektronix).

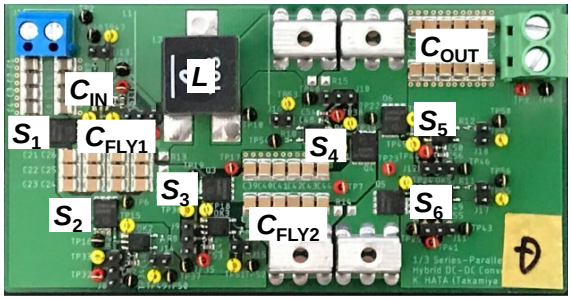

Fig. 9. Prototype of the proposed ADPH converter.

TABLE I. Circuit Components and Parameters.

Parameters	Value and Design Selection
Input voltage V_{IN}	22 – 32 V (24 $V_{nominal}$)
Output voltage V_{OUT}	13 V
Output current I_{OUT}	15 A_{max}
Output power P_{OUT}	200 W_{max}
Switching frequency	100 kHz
Power MOSFETs $S_{1\text{–}6}$	40 V, $R_{DS(on),max}$: 2.2 mΩ, BSC022N04LS6, Infineon
Input capacitor C_{IN}	80 µF (10 µF × 8), X7S, GCM32EC71H106KA03, Murata
Flying capacitors $C_{FLY1,2}$	264 µF (22 µF × 12), X7R, GRM32ER71E226KE15, Murata
Output capacitor C_O	264 µF (22 µF × 12), X7R, GRM32ER71E226KE15, Murata
Inductor L	10 µH, DCR: 6.8 mΩ, XAL1510-103, Coilcraft

B. Measurement results

Fig. 10 shows the measured efficiency of the proposed ADPH and conventional buck converters under conditions of V_{IN} = 24 V, V_{OUT} = 13 V, M = 13/24, and f_{SW} = 100 kHz. The peak efficiency of both converters is 97.4 %, but the conventional buck converter achieved this in the range of I_{OUT} = 7 – 8 A and the proposed ADPH converter was achieved in the range of I_{OUT} = 7 – 11 A. At I_{OUT} = 15 A, the efficiency is 97.0 % and 96.7 % in the proposed and the conventional converters, respectively, increasing the improvement in efficiency to 0.3 %. Under these conditions, it is expected that the superiority of the proposed ADPH converter will be confirmed in the range where the output current is even larger, so future measurements will be carried out as a future work.

The measured inductor DC current I_L is indicated in Fig. 11. In the conventional buck converter, I_L has the same value as I_{OUT}, but in the proposed ADPH converter, I_L can be drastically reduced from I_{OUT}. As a result, the inductor conduction loss can be significantly suppressed as shown in Fig. 12. This result helps to cool the coil and suggests that it is advantageous when using an inductor with a large DCR.

V. Conclusions

An always-dual-path hybrid (ADPH) DC-DC converter is proposed to achieve high efficiency at the most commonly used 2:1 step-down ratio by reducing the inductor current. In the measurement, the peak efficiency of the proposed 24 V-

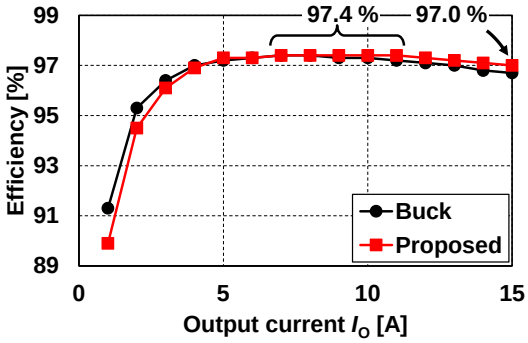

Fig. 10. Measured efficiency comparison between proposed ADPH converter and conventional buck converter.

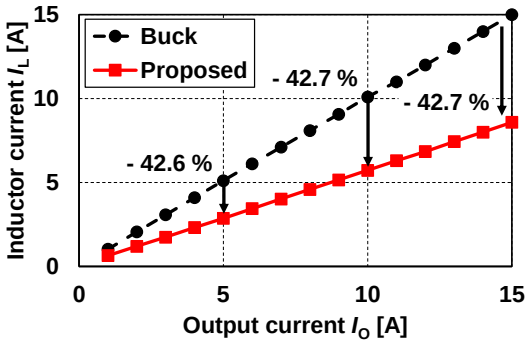

Fig. 11. Measured inductor DC current comparison between proposed ADPH converter and conventional buck converter.

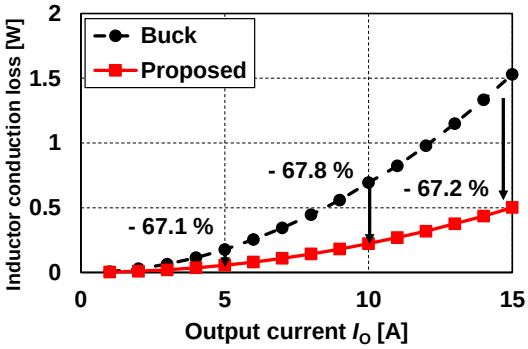

Fig. 12. Calculated inductor conduction loss comparison between proposed ADPH converter and conventional buck converter based on measured inductor DC current.

to-13 V converter is 97.4 % at 146 W, and the inductor conduction loss is reduced by 67.2 % by reducing the inductor DC current by 42.7 %.

As future tasks, we will select power switches suitable for the proposed ADPH converter and carry out a demonstration experiment using an inductor with a larger DCR.

Acknowledgment

This work was partly supported by Toyota Industries Corporation and JSPS KAKENHI Grant Number 20K14710. The authors would like to thank Sadanori Suzuki of Toyota Industries Corporation for the technical discussion on the converter design.

References

[1] E. Candan, A. Stillwell, N. C. Brooks, R. A. Abramson, J. Strydom, and R. C. N. Pilawa-Podgurski, "A 6-level Flying Capacitor Multi-level Converter for Single Phase Buck-type Power Factor Correction," in Proc. IEEE Applied Power Electronics Conference and Exposition (APEC), 2019, pp. 1180-1187.

[2] T. Xie, R. Das, G. Seo, D. Maksimovic, and H-P. Le, "Multiphase Control for Robust and Complete Soft-charging Operation of Dual Inductor Hybrid Converter," in Proc. IEEE Applied Power Electronics Conference and Exposition (APEC), 2019, pp. 1-5.

[3] M. Halamicek, T. McRae, N. Vukadinović, and A. Prodić, "Modulation Scheme for an Effective Increase in the Number of Levels of DC-DC Multi-Level Flying Capacitor Converters," in Proc. IEEE Applied Power Electronics Conference and Exposition (APEC), 2019, pp. 45-49.

[4] J. S. Rentmeister and J. T. Stauth, "Zero Voltage Switching for Flying Capacitor Multilevel Converters at Nominal Conversion Ratios," in Proc. IEEE Applied Power Electronics Conference and Exposition (APEC), 2019, pp. 30-36.

[5] Y. Lei, W. Liu, and R. C. N. Pilawa-Podgurski, "An Analytical Method to Evaluate and Design Hybrid Switched-Capacitor and Multilevel Converters," IEEE Transactions on Power Electronics, vol. 33, no. 3, pp. 2227-2240, March 2018.

[6] F. Bez, G. Bonanno, L. Corradini, and C. Garbossa, "Control technique for reliable operation of the synchronous series capacitor tapped inductor converter," in Proc. IEEE Applied Power Electronics Conference and Exposition (APEC), 2018, pp. 113-120.

[7] S. Biswas and D. Reusch, "GaN Based Switched Capacitor Three-Level Buck Converter with Cascaded Synchronous Bootstrap Gate Drive Scheme," in Proc. IEEE Energy Conversion Congress and Exposition (ECCE), 2018, pp. 3490-3496.

[8] O. Kirshenboim and M. M. Peretz, "High-Efficiency Nonisolated Converter With Very High Step-Down Conversion Ratio," IEEE Transactions on Power Electronics, vol. 32, no. 5, pp. 3683-3690, May 2017.

[9] P. S. Shenoy, O. Lazaro, R. Ramani, M. Amaro, W. Wiktor, J. Khayat, and B. Lynch, "A 5 MHz, 12 V, 10 A, monolithically integrated two-phase series capacitor buck converter," in Proc. IEEE Applied Power Electronics Conference and Exposition (APEC), 2016, pp. 66-72.

[10] P. S. Shenoy, M. Amaro, J. Morroni, and D. Freeman, "Comparison of a Buck Converter and a Series Capacitor Buck Converter for High-Frequency, High-Conversion-Ratio Voltage Regulators," IEEE Transactions on Power Electronics, vol. 31, no. 10, pp. 7006-7015, Oct. 2016.

[11] N. Vukadinović, A. Prodić, B. A. Miwa, C. B. Arnold, and M. W. Baker, "Extended wide-load range model for multi-level Dc-Dc converters and a practical dual-mode digital controller," in Proc. IEEE Applied Power Electronics Conference and Exposition (APEC), 2016, pp. 1597-1602.

[12] G. Seo and H-P. Le, "S-Hybrid Step-Down DC-DC Converter-Analysis of Operation and Design Considerations," IEEE Transactions on Industrial Electronics, vol. 67, no. 1, pp. 265–275, Jan. 2020.

[13] G. Seo and H-P. Le, "An inductor-less hybrid step-down DC-DC converter architecture for future smart power cable," in Proc. IEEE Applied Power Electronics Conference and Exposition (APEC), 2017, pp. 247-253.

[14] Y. Huh, S. Hong, and G. Cho, "A Hybrid Structure Dual-Path Step-Down Converter With 96.2% Peak Efficiency Using 250-mΩ Large-DCR Inductor," IEEE Journal of Solid-State Circuits, vol. 54, no. 4, pp. 959-967, April 2019.

[15] K. Hata, Y. Yamauchi, T. Sai, T. Sakurai, and M. Takamiya, "48V-to-12V Dual-Path Hybrid DC-DC Converter," in Proc. IEEE Applied Power Electronics Conference and Exposition (APEC), 2020, pp. 2279-2284.

[16] X. Liu, P. K. T. Mok, J. Jiang, and W. H. Ki, "Analysis and design considerations of integrated 3-level buck converters," IEEE Transactions on Circuits and Systems I: Regular Papers, vol. 63, no. 5, pp. 671–682, May 2016.

[17] Y. Yamauchi, T. Sai, T. Sakurai, and M. Takamiya, "Modeling of 3-Level Buck Converters in Discontinuous Conduction Mode for Stand-by Mode Power Supply," in Proc. IEEE International Symposium for Circuits and Systems (ISCAS), 2017, pp. 1282-1285.